

Article

Not peer-reviewed version

---

# A Comprehensive Error Modeling and On-Field Calibration Method for HRG SINS by Tumbling the Hexahedron

---

[Yuanxi Li](#), [Zhennan Wei](#)<sup>\*</sup>, [Shunqing Ren](#), [Qingshuang Zeng](#)

Posted Date: 17 November 2025

doi: 10.20944/preprints202511.1195.v1

Keywords: strapdown inertial navigation system; hemispherical resonator gyroscope; on-field calibration



Preprints.org is a free multidisciplinary platform providing preprint service that is dedicated to making early versions of research outputs permanently available and citable. Preprints posted at Preprints.org appear in Web of Science, Crossref, Google Scholar, Scilit, Europe PMC.

Copyright: This open access article is published under a [Creative Commons CC BY 4.0 license](#), which permit the free download, distribution, and reuse, provided that the author and preprint are cited in any reuse.

Disclaimer/Publisher's Note: The statements, opinions, and data contained in all publications are solely those of the individual author(s) and contributor(s) and not of MDPI and/or the editor(s). MDPI and/or the editor(s) disclaim responsibility for any injury to people or property resulting from any ideas, methods, instructions, or products referred to in the content.

Article

# A Comprehensive Error Modeling and On-Field Calibration Method for HRG SINS by Tumbling the Hexahedron

Yuanxi Li, Zhennan Wei \*, Shunqing Ren and Qingshuang Zeng

Harbin Institute of Technology, Harbin, China

\* Correspondence: wzn@hit.edu.cn

## Highlights

1. A comprehensive error model is developed to couple hexahedron structural errors with SINS calibration accuracy.
2. Novel 24-position and 48-tumble schemes enable simultaneous identification of accelerometers and gyro errors.
3. Experimental results confirm higher calibration accuracy and reduce fixture precision requirements.
4. The approach reduces demands for mechanical error tolerance towards the hexahedral fixture, and reduce on-field calibration cost, finally enables reliable, high-precision calibration for HRG SINS.

## What are the main findings?

- A comprehensive on-field calibration method for HRG SINS is developed, incorporating hexahedral structural errors.
- The proposed 24-position accelerometer calibration and 48-rotation gyro calibration schemes enable simultaneous identification of sensor biases, scale factor errors, installation misalignments, and fixture-induced errors.

## What are the implications of the main findings?

- The method significantly improves calibration accuracy of both accelerometers and HRGs compared to traditional approaches.
- It relaxes the mechanical precision requirements of the hexahedral fixture, reducing the cost and complexity of on-field calibration.

## Abstract

On-field calibration for SINS often uses right hexahedron, but the influence of the structure errors, such as mutual position tolerances towards parallelism or the perpendicularity of two arbitrary planes of the hexahedron, on the calibration accuracy is often neglected. In this paper, a hexahedron structure error model and a comprehensive corresponding SINS calibration error model are developed based on hemispherical resonator gyroscope (HRGs). The proposed method introduces the comprehensive hexahedron errors through defining the normal vectors of the exterior surfaces of the hexahedron. A 24-position calibration scheme is designed to identify accelerometer-related errors, while a 48-rotation scheme is developed to identify gyro-related errors. The complete calibration procedure enables simultaneous identification of hexahedron structure errors, installation misalignments, scale factor errors, and biases. Experimental validation is conducted using a high-precision three-axis turntable, which simulates the hexahedron structure errors. The results show that the proposed method significantly improves the calibration accuracy of both accelerometers and HRGs compared with traditional methods. Furthermore, it reduces the accuracy requirements for the hexahedron structure, thus lowering the cost of SINS on-field calibration.

**Keywords:** strapdown inertial navigation system; hemispherical resonator gyroscope; on-field calibration

---

## 1. Introduction

The strapdown inertial navigation system (SINS) plays a critical role in aerospace, marine, and autonomous navigation applications, where practical navigation accuracy strongly depends on the precise calibration of the inertial measurement unit. The inertial measurement unit typically consists of three accelerometers and three gyroscopes mounted along mutually orthogonal axes. Calibration aims to determine and compensate for the systematic errors of these sensors, such as biases, scale factors, and misalignment errors, thereby ensuring the integrity of navigation performance.

Early research on SINS calibration, such as the work by Bailey at NASA [1], established the theoretical framework of strapdown calibration and alignment using gravity and Earth's rotation as reference inputs. Later, Nassar [2] improved the INS error modeling approach and emphasized the importance of systematic calibration for accurate navigation. With the development of low-cost and medium-precision MEMS-based IMUs, calibration techniques have evolved rapidly to address the growing needs for accuracy and flexibility in field environments.

Traditional calibration methods generally employ a regular hexahedral fixture to mount the SINS. The cube is sequentially placed in multiple orientations on a horizontal reference slab to generate different known inertial inputs, allowing the estimation of sensor biases, scale factors, and misalignment angles [3–5]. Rahimi et al. [6] proposed a multi-position calibration method using rotations to estimate the cross-coupling and scale factor errors of marine-grade IMUs, while Vavilova [7] summarized the calibration problem as a fundamental step in inertial navigation to establish an accurate sensor error model.

However, most conventional methods assume that the hexahedral fixture is geometrically ideal. In practice, machining tolerances, assembly misalignments, and nonorthogonalities between faces introduce hexahedral structural errors, which lead to deviations in the attitude relationships between the calibration positions. As a result, these unmodeled fixture errors can significantly degrade calibration accuracy, especially for high-precision SINS employing hemispherical resonator gyros (HRGs) [8–10].

In view of the problem that conventional on-field calibration approaches for strapdown inertial navigation systems typically treat the hexahedral fixture as geometrically perfect, overlooking the potential structural errors inherent in the device. Such unaccounted-for errors can substantially compromise the calibration precision of the SINS error model. In this study, we develop a hexahedral structural error model along with a comprehensive calibration error model for the strapdown inertial navigation systems based on hemispherical resonator gyroscope to field. The proposed approach incorporates the complete set of hexahedral errors by defining the normal vector of each face. We proposed a 24-position calibration protocol for accelerometer error identification, and a 48-rotation procedure to determine gyroscope-related errors. This calibration allows for the simultaneous estimation of hexahedral structural errors, installation misalignments, scale factor deviations, and biases. Experimental verification is carried out on a high-precision three-axis turntable which simulated the hexahedral structural deviations. The results demonstrate that the proposed method substantially enhances the calibration accuracy for both accelerometers and HRGs compared to traditional approaches. Additionally, it relaxes the mechanical precision requirements of the hexahedral fixture, thereby reducing the overall cost of SINS on-field calibration.

## 2. The Calibration System and Establishment of Coordinate Systems

Traditional on-field calibration of Strapdown Inertial Navigation Systems typically employs a regular hexahedral fixture. The gravity-induced specific force and the Earth's rotation rate are used as two vectors of motion parameters, and the hexahedron is tumbled to provide different excitations

for the SINS. However, traditional SINS on-field calibration methods generally neglect the structural errors of the hexahedron. In practice, mutual position errors between the faces of the hexahedron, such as deviations in parallelism and perpendicularity, introduce additional errors during the calibration process, thereby affecting the identification accuracy of the SINS error model.

As shown in Figure 1, the strapdown inertial navigation systems based on hemispherical resonator gyroscope is calibrated by placing the hexahedron on the on-field slab. A located block is mounted on the slab to provide positioning. the azimuth of the edge of the located block is precise determined, therefore, providing precise components of the turn rate of the Earth. The hexahedron is placed tightly against the located block and then rotated on the slab, ensuring that one face of the hexahedron is placed tightly against the located block after each rotation. By changing the orientation of the hexahedron, the input of the SINS is varied. Different attitude transformations are designed to achieve the on-field calibration of the SINS.

To accurately analyze the error propagation mechanism of the strapdown inertial navigation system, several auxiliary coordinate systems are established as follows. The navigation coordinate system  $o_n x_n y_n z_n$  is defined such that its three axes point toward the local east, local north, and local up directions, respectively. The slab coordinate system  $o_1 x_1 y_1 z_1$  is defined with its origin  $o_1$  located on the slab. The  $o_1 z_1$  axis is parallel to the normal vector of the slab, pointing up and perpendicular to the slab surface. The hexahedron coordinate system  $o_b x_b y_b z_b$  is rigidly attached to the strapdown inertial navigation system's hexahedral structure. These coordinate systems together provide a consistent spatial reference framework that serves as the foundation for subsequent calibration error analysis and the establishment of the system's comprehensive error model.

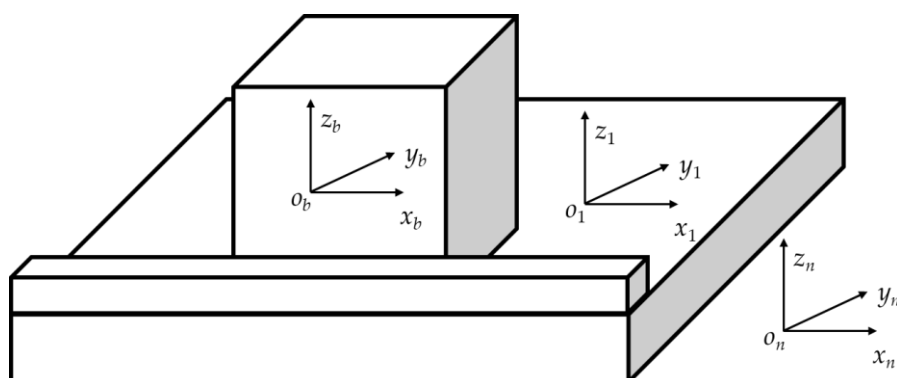


Figure 1. SINS on-field calibration.

## 2. Error Mechanism Analysis.

To improve the on-field calibration accuracy of the strapdown inertial navigation system based on hemispherical resonator gyroscope, it is necessary to analyze the error mechanisms involved in the system's on-field calibration. Based on this analysis, the on-field calibration error model of the system that includes all error sources is established.

### 2.1. Definition of Mutual Position Error of Hexahedron

To improve the accuracy of on-field calibration for strapdown inertial navigation systems based on hemispherical resonator gyroscopes, it is necessary to analyze the effects of the hexahedral structural errors, which are often neglected in traditional calibration methods. Based on this analysis, an accurate error model that incorporates the complete hexahedral calibration errors through normal vectors is established.

The hexahedron coordinate system is defined by the inner normal vector of the first face, the normal vector of the edge shared by the first and second faces, and the projection of the inner normal vector of the second face onto the plane of the first face. It is assumed that the angular deviations between the actual hexahedron and the ideal standard hexahedron are small.

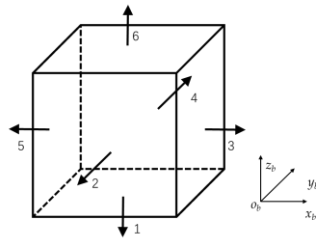


**Figure 2.** The hexahedral structure.

The outward normal vector of the first face of the hexahedron is defined as  $n_1$ . The outward normal vector of the second face,  $n_2$ , is determined based on its perpendicularity deviation  $\Delta\theta_{x2}$  relative to  $n_1$ . Using  $n_1$  and  $n_2$  as references, the outward normal vector of the third face,  $n_3$ , is defined, and the remaining faces are defined sequentially in the same manner.

Through this definition, nine parameters are employed in this paper to comprehensively represent the parallelism and perpendicularity errors among the faces of the hexahedron, providing a fundamental basis for the subsequent establishment of the SINS calibration error model.

The outward normal vectors of the hexahedron surfaces in the hexahedron coordinate system are defined as shown in eq. (1).

$$\begin{aligned} n_1 &: [0 \ 0 \ -1]^T & n_2 &: [0 \ -1 \ \Delta\theta_{x2}]^T & n_3 &: [1 \ -\Delta\theta_{z3} \ \Delta\theta_{y3}]^T \\ n_4 &: [\Delta\theta_{z4} \ 1 \ -\Delta\theta_{x4}]^T & n_5 &: [-1 \ \Delta\theta_{z5} \ -\Delta\theta_{y5}]^T & n_6 &: [-\Delta\theta_{y6} \ \Delta\theta_{x6} \ 1]^T \end{aligned} \quad (1)$$

## 2.2. Error Analysis of the Strapdown Inertial Navigation System

Ideally, the three accelerometers and three hemispherical resonator gyroscopes of the strapdown inertial navigation system are perfectly aligned with the three axes of the hexahedron coordinate system. In practice, however, assembly imperfections introduce installation errors between the sensitive axes of the accelerometers and HRGs and the axes of the hexahedron coordinate system. In this study, these installation errors are expressed in vector form. The normal vectors of the sensitive axes of the three accelerometers and the three HRGs, represented in the hexahedron coordinate system, are shown in eq. (2).

$$\begin{aligned} s^x &= [1 \ \alpha_{z1} \ -\alpha_{y1}]^T & g^x &= [1 \ \alpha_z \ -\alpha_y]^T \\ s^y &= [-\beta_{z1} \ 1 \ \beta_{x1}]^T & g^y &= [-\beta_z \ 1 \ \beta_x]^T \\ s^z &= [\gamma_{y1} \ -\gamma_{x1} \ 1]^T & g^z &= [\gamma_y \ -\gamma_x \ 1]^T \end{aligned} \quad (2)$$

The three accelerometers and three hemispherical resonator gyroscopes of the strapdown inertial navigation system also exhibit scale factor errors and bias errors. The output error equations of the three accelerometers are shown in eq. (3).

$$\begin{bmatrix} N_x^a \\ N_y^a \\ N_z^a \end{bmatrix} = \begin{bmatrix} 1 + \Delta K_{ax} & 0 & 0 \\ 0 & 1 + \Delta K_{ay} & 0 \\ 0 & 0 & 1 + \Delta K_{az} \end{bmatrix} \begin{bmatrix} f_x^b \\ f_y^b \\ f_z^b \end{bmatrix} + \begin{bmatrix} B_{ax} \\ B_{ay} \\ B_{az} \end{bmatrix} + \begin{bmatrix} n_{ax} \\ n_{ay} \\ n_{az} \end{bmatrix} \quad (3)$$

The output error equations of the three HRGs are shown in eq. (4).

$$\begin{bmatrix} N_x^g \\ N_y^g \\ N_z^g \end{bmatrix} = \begin{bmatrix} 1 + \Delta K_{gx} & 0 & 0 \\ 0 & 1 + \Delta K_{gy} & 0 \\ 0 & 0 & 1 + \Delta K_{gz} \end{bmatrix} \begin{bmatrix} \omega_{ibx}^b \\ \omega_{iby}^b \\ \omega_{ibz}^b \end{bmatrix} + \begin{bmatrix} B_{gx} \\ B_{gy} \\ B_{gz} \end{bmatrix} + \begin{bmatrix} n_{gx} \\ n_{gy} \\ n_{gz} \end{bmatrix} \quad (4)$$

## 2.3. Error Analysis of the Slab Coordinate System

In the initial position, the slab coordinate system coincides with the navigation coordinate system. However, due to factors such as fixture errors of the slab, there exist leveling errors  $\Delta\theta_{x0}$  and

$\Delta\theta_{y0}$ , and horizontal zero offset error  $\Delta\gamma_0$  between the slab coordinate system and the navigation coordinate system. The attitude matrix between the navigation coordinate system and the slab coordinate system is given in eq. (5).

$$\mathbf{C}_n^1 = \begin{bmatrix} 1 & \Delta\gamma_0 & 0 \\ -\Delta\gamma_0 & 1 & 0 \\ 0 & 0 & 1 \end{bmatrix} \begin{bmatrix} 1 & 0 & -\Delta\theta_{y0} \\ 0 & 1 & \Delta\theta_{x0} \\ \Delta\theta_{y0} & -\Delta\theta_{x0} & 1 \end{bmatrix} \quad (5)$$

#### 2.4. The Motion Parameters Inputs of Accelerometer and HRGs

The specific force generated by gravitational acceleration in the navigation coordinate system is  $\mathbf{g}^0 = [0 \ 0 \ 1]^T$ . Then, its representation in the slab coordinate system is given by

$$\mathbf{g}^1 = (\mathbf{C}_n^1)^T \begin{bmatrix} 0 \\ 0 \\ 1 \end{bmatrix} = \begin{bmatrix} -\Delta\theta_{y0} \\ \Delta\theta_{x0} \\ 1 \end{bmatrix} \quad (6)$$

The Earth's rotation angular velocity expressed in the navigation coordinate system is  $[0 \ \omega_{ie} \cos L \ \omega_{ie} \sin L]^T$ .

The transformation matrix from the navigation coordinate system to the slab coordinate system is shown in eq. (5). The Earth's rotation angular velocity expressed in the slab coordinate system is shown in eq. (7).

$$\boldsymbol{\omega} = (\mathbf{C}_n^1)^T \begin{bmatrix} 0 \\ \omega_{ie} \cos L \\ \omega_{ie} \sin L \end{bmatrix} = \begin{bmatrix} \omega_{ie} \cos L \cdot \Delta\gamma_0 - \omega_{ie} \sin L \cdot \Delta\theta_{y0} \\ \omega_{ie} \cos L + \omega_{ie} \sin L \cdot \Delta\theta_{x0} \\ \omega_{ie} \sin L - \omega_{ie} \cos L \cdot \Delta\theta_{x0} \end{bmatrix} \quad (7)$$

During the on-field calibration of the SINS, the method involves placing two faces of the hexahedron tightly against the slab and the located block, followed by tumbling the hexahedron for calibration. After each tumble, it is ensured that two faces of the hexahedron remain tightly placed against the slab and the located block.

For different calibration positions, traditional on-field calibration of the SINS typically treats it as a rotation around the three axes of the coordinate system to achieve the desired calibration position. However, due to structural errors in the hexahedron, such an equivalent rotation introduces significant errors into the on-field calibration of the SINS.

This paper addresses the issue using a vector-based approach. During the on-field calibration of the SINS, the outward normal vector of the face of the hexahedron placed tightly against the slab is opposite to the z-axis direction of the slab coordinate system, while the outward normal vector of the face of the hexahedron placed tightly against the located block is opposite to the y-axis direction of the slab coordinate system.

Therefore, the unit vectors of the three axes of the slab coordinate system can be expressed in the hexahedron coordinate system. The resulting transformation matrix is given by eq. (8).

$$\mathbf{C}_0 = \begin{bmatrix} (\mathbf{v}_B \times \mathbf{v}_A)^T \\ (\mathbf{v}_B \times \mathbf{v}_A \times \mathbf{v}_A)^T \\ ((\mathbf{v}_B \times \mathbf{v}_A) \times (\mathbf{v}_B \times \mathbf{v}_A \times \mathbf{v}_A))^T \end{bmatrix} \quad (8)$$

where,  $\mathbf{v}_A$  is the outward normal vector of the face of the hexahedron placed tightly against the slab, and  $\mathbf{v}_B$  is the outward normal vector of the face of the hexahedron placed tightly against the located block. Normalize the matrix  $\mathbf{C}_0$  to obtain the transformation matrix  $\mathbf{C}_1$ .

Taking the position where the first face of the hexahedron is placed tightly against the slab and the fifth face is placed tightly against the located block as an example. The transformation matrix is shown in eq. (9).

$$C_1 = \begin{bmatrix} -\Delta\theta_{z5} & -1 & 0 \\ 1 & -\Delta\theta_{z5} & 0 \\ 0 & 0 & 1 \end{bmatrix} \quad (9)$$

The input specific forces of the three accelerometers are shown in eq. (10).

$$\begin{aligned} \alpha_x^{1.5} &= \begin{bmatrix} -\Delta\theta_{y0} & \Delta\theta_{x0} & 1 \end{bmatrix} \cdot \begin{bmatrix} -\Delta\theta_{z5} & -1 & 0 \\ 1 & -\Delta\theta_{z5} & 0 \\ 0 & 0 & 1 \end{bmatrix} \cdot \begin{bmatrix} 1 & \alpha_{z1} & -\alpha_{y1} \end{bmatrix}^T = \Delta\theta_{x0} - \alpha_{y1} \\ \alpha_y^{1.5} &= \begin{bmatrix} -\Delta\theta_{y0} & \Delta\theta_{x0} & 1 \end{bmatrix} \cdot \begin{bmatrix} -\Delta\theta_{z5} & -1 & 0 \\ 1 & -\Delta\theta_{z5} & 0 \\ 0 & 0 & 1 \end{bmatrix} \cdot \begin{bmatrix} -\beta_{z1} & 1 & \beta_{x1} \end{bmatrix}^T = \Delta\theta_{y0} + \beta_{x1} \\ \alpha_z^{1.5} &= \begin{bmatrix} -\Delta\theta_{y0} & \Delta\theta_{x0} & 1 \end{bmatrix} \cdot \begin{bmatrix} -\Delta\theta_{z5} & -1 & 0 \\ 1 & -\Delta\theta_{z5} & 0 \\ 0 & 0 & 1 \end{bmatrix} \cdot \begin{bmatrix} \gamma_{y1} & -\gamma_{x1} & 1 \end{bmatrix}^T = 1 \end{aligned} \quad (10)$$

Due to the small magnitude of the Earth's rotation angular velocity, it is insufficient to provide effective inertial vector inputs for the three HRGs of the SINS. In this paper, a method is proposed in which the hexahedron is rotated on the slab to provide inertial vector inputs for the HRGs.

When the first face of the hexahedron is placed tightly against the slab, the projections of the second, third, fourth, and fifth faces onto the slab are shown in eq. (11).

$$n'_2 : [0 \ -1 \ 0] \quad n'_3 : [1 \ -\Delta\theta_{z3} \ 0] \quad n'_4 : [\Delta\theta_{z4} \ 1 \ 0] \quad n'_5 : [-1 \ \Delta\theta_{z5} \ 0] \quad (11)$$

The tumble angles of the hexahedron can be determined through the projections of the outward normal vectors of the faces onto the slab.

Taking the example where the first face of the hexahedron is placed tightly against the slab, and it tumbles from the second face placed tightly against the located block to the fifth face placed tightly against the located block.

At this point, the angular velocity inputs for the three HRGs of the SINS are composed of the tumble of the hexahedron and the Earth's rotational angular velocity.

The angular velocity input caused by the tumble of the hexahedron results in the HRG output, which, after integration, is expressed as shown in eq. (12).

$$\begin{aligned} \alpha_x^{1.2.5} &= \int [0 \ 0 \ \omega] \cdot \begin{bmatrix} 1 & \alpha_z & -\alpha_y \end{bmatrix}^T dt = \left[ 0 \ 0 \ \frac{\pi}{2} + \Delta\theta_{z5} \right] \cdot \begin{bmatrix} 1 & \alpha_z & -\alpha_y \end{bmatrix}^T = -\alpha_y \cdot \left( \frac{\pi}{2} + \Delta\theta_{z5} \right) \\ \alpha_y^{1.2.5} &= \int [0 \ 0 \ \omega] \cdot \begin{bmatrix} -\beta_z & 1 & \beta_x \end{bmatrix}^T dt = \left[ 0 \ 0 \ \frac{\pi}{2} + \Delta\theta_{z5} \right] \cdot \begin{bmatrix} -\beta_z & 1 & \beta_x \end{bmatrix}^T = \beta_x \cdot \left( \frac{\pi}{2} + \Delta\theta_{z5} \right) \\ \alpha_z^{1.2.5} &= \int [0 \ 0 \ \omega] \cdot \begin{bmatrix} \gamma_y & -\gamma_x & 1 \end{bmatrix}^T dt = \left[ 0 \ 0 \ \frac{\pi}{2} + \Delta\theta_{z5} \right] \cdot \begin{bmatrix} \gamma_y & -\gamma_x & 1 \end{bmatrix}^T = \frac{\pi}{2} + \Delta\theta_{z5} \end{aligned} \quad (12)$$

The Earth's rotation angular velocity expressed in the slab coordinate system is shown in eq. (7). The angular velocity input caused by the tumble of the hexahedron and the Earth's rotational angular velocity results in the HRG output, which, after integration, is expressed as shown in eq. (13).

$$\alpha_z^{1.2.5} = \frac{\pi}{2} + \Delta\theta_{z5} + \omega_e T \sin L \quad (13)$$

### 2.5. Total Error Model for Calibration

This paper analyzes all error sources in the on-field calibration of the SINS, including slab errors, and hexahedron structural errors, installation errors, scale factor errors, and biases of the three HRGs and three accelerometers. An on-field calibration error model of the SINS was established for different SINS positions.

When the sixth face of the hexahedron is placed tightly against the slab and the fourth face is placed tightly against the located block, the error model of the three accelerometers of the SINS is given by eq. (13).

$$\begin{bmatrix} N_x^a \\ N_y^a \\ N_z^a \end{bmatrix} = \begin{bmatrix} (1 + \Delta K_{ax})(-\Delta\theta_{y0} + \Delta\theta_{y6} + \alpha_{y1}) + B_{ax} + n_{ax} \\ (1 + \Delta K_{ay})(-\Delta\theta_{x0} + \Delta\theta_{x6} + \beta_{x1}) + B_{ay} + n_{ay} \\ -1 - \Delta K_{az} + B_{az} + n_{az} \end{bmatrix} \tag{13}$$

When the second face of the hexahedron is placed tightly against the slab, and the hexahedron tumbles from the third face placed tightly against the located block to the sixth face placed tightly against the located block, the error model of the HRGs is shown in eq. (14).

$$\begin{bmatrix} N_x^g \\ N_y^g \\ N_z^g \end{bmatrix} = \begin{bmatrix} (1 + \Delta K_{gx})\alpha_z \cdot \frac{\pi}{2} + T \cdot B_{gx} + n_{gx} \\ (1 + \Delta K_{gy})\left(\frac{\pi}{2} - \Delta\theta_{y3} + \Delta\theta_{y6} + \omega_{te} \sin L \cdot T\right) + T \cdot B_{gy} + n_{gy} \\ (1 + \Delta K_{gz})(\Delta\theta_{x2} - \gamma_x) \cdot \frac{\pi}{2} + T \cdot B_{gz} + n_{gz} \end{bmatrix} \tag{14}$$

### 3. Identification of Error Parameters of SINS.

To identify the error model coefficients associated with the accelerometers in the strapdown inertial navigation system, a 24-position SINS calibration method was designed. In this approach, each face of the hexahedron is sequentially placed tightly against the slab, followed by aligning another face with the horizontal reference surface of the slab.

This procedure can be interpreted as orienting the  $x_b$ ,  $y_b$ , and  $z_b$  axes of the hexahedron coordinate system along the upward and downward directions, and then sequentially tumbling them while keeping them placed tightly against the positioning plane of the located block.

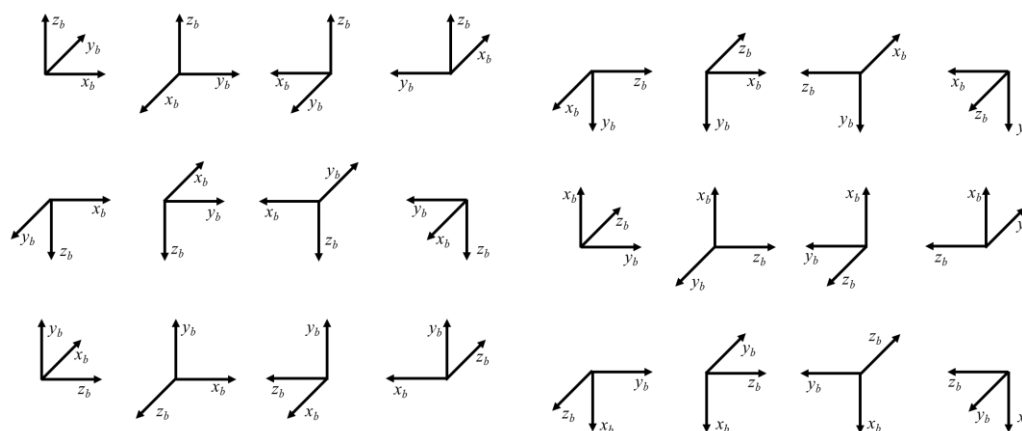


Figure 3. 24 position SINS calibration method

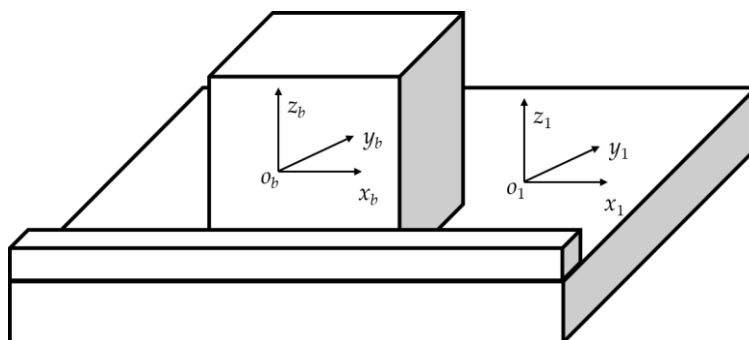


Figure 4. Hexahedral structure calibration.

First, the first face of the hexahedron is placed tightly against the slab, followed sequentially by placing the second, third, fourth, and fifth faces tightly against the located block. When the second face of the hexahedron is placed tightly against the located block, the specific forces of the three accelerometers in the slab coordinate system are calculated as:

$$\begin{aligned}\alpha_x^{1,2} &= [-\Delta\theta_{y0} \quad \Delta\theta_{x0} \quad 1] \cdot [1 \quad \alpha_{z1} \quad -\alpha_{y1}]^T = -\Delta\theta_{y0} - \alpha_{y1} \\ \alpha_y^{1,2} &= [-\Delta\theta_{y0} \quad \Delta\theta_{x0} \quad 1] \cdot [-\beta_{z1} \quad 1 \quad \beta_{x1}]^T = \Delta\theta_{x0} + \beta_{x1} \\ \alpha_z^{1,2} &= [-\Delta\theta_{y0} \quad \Delta\theta_{x0} \quad 1] \cdot [\gamma_{y1} \quad -\gamma_{x1} \quad 1]^T = 1\end{aligned}\quad (15)$$

When the fourth face of the hexahedron is placed tightly against the located block, the specific forces of the three accelerometers are calculated as

$$\begin{aligned}\alpha_x^{1,4} &= [-\Delta\theta_{y0} \quad \Delta\theta_{x0} \quad 1] \cdot \begin{bmatrix} -1 & \Delta\theta_{z4} & 0 \\ -\Delta\theta_{z4} & -1 & 0 \\ 0 & 0 & 1 \end{bmatrix} \cdot [1 \quad \alpha_{z1} \quad -\alpha_{y1}]^T = \Delta\theta_{y0} - \alpha_{y1} \\ \alpha_y^{1,4} &= [-\Delta\theta_{y0} \quad \Delta\theta_{x0} \quad 1] \cdot \begin{bmatrix} -1 & \Delta\theta_{z4} & 0 \\ -\Delta\theta_{z4} & -1 & 0 \\ 0 & 0 & 1 \end{bmatrix} \cdot [-\beta_{z1} \quad 1 \quad \beta_{x1}]^T = -\Delta\theta_{x0} + \beta_{x1} \\ \alpha_z^{1,4} &= [-\Delta\theta_{y0} \quad \Delta\theta_{x0} \quad 1] \cdot \begin{bmatrix} -1 & \Delta\theta_{z4} & 0 \\ -\Delta\theta_{z4} & -1 & 0 \\ 0 & 0 & 1 \end{bmatrix} \cdot [\gamma_{y1} \quad -\gamma_{x1} \quad 1]^T = 1\end{aligned}\quad (16)$$

When the third face of the hexahedron is placed tightly against the located block, the specific forces of the three accelerometers are calculated as

$$\begin{aligned}\alpha_x^{1,3} &= [-\Delta\theta_{y0} \quad \Delta\theta_{x0} \quad 1] \cdot \begin{bmatrix} \Delta\theta_{z3} & 1 & 0 \\ -1 & \Delta\theta_{z3} & 0 \\ 0 & 0 & 1 \end{bmatrix} \cdot [1 \quad \alpha_{z1} \quad -\alpha_{y1}]^T = -\Delta\theta_{x0} - \alpha_{y1} \\ \alpha_y^{1,3} &= [-\Delta\theta_{y0} \quad \Delta\theta_{x0} \quad 1] \cdot \begin{bmatrix} \Delta\theta_{z3} & 1 & 0 \\ -1 & \Delta\theta_{z3} & 0 \\ 0 & 0 & 1 \end{bmatrix} \cdot [-\beta_{z1} \quad 1 \quad \beta_{x1}]^T = -\Delta\theta_{y0} + \beta_{x1} \\ \alpha_z^{1,3} &= [-\Delta\theta_{y0} \quad \Delta\theta_{x0} \quad 1] \cdot \begin{bmatrix} \Delta\theta_{z3} & 1 & 0 \\ -1 & \Delta\theta_{z3} & 0 \\ 0 & 0 & 1 \end{bmatrix} \cdot [\gamma_{y1} \quad -\gamma_{x1} \quad 1]^T = 1\end{aligned}\quad (17)$$

Using the 24-position strapdown inertial navigation system error calibration method designed in this paper, a total of 72 sets of test data were obtained. From these data, we have

$$\begin{bmatrix} a_x^{1,2} \\ a_y^{1,2} \\ a_z^{1,2} \\ a_x^{1,5} \\ \vdots \\ a_z^{5,4} \\ a_x^{5,1} \\ a_y^{5,1} \\ a_x^{5,1} \end{bmatrix} = A \cdot \begin{bmatrix} 1 + \Delta K_{ax} \\ (1 + \Delta K_{ax})\Delta\theta_{x0} \\ (1 + \Delta K_{ax})\Delta\theta_{y0} \\ (1 + \Delta K_{ax})\Delta\theta_{y6} \\ (1 + \Delta K_{ax})\Delta\theta_{z4} \\ (1 + \Delta K_{ax})\alpha_{y1} \\ (1 + \Delta K_{ax})\alpha_{z1} \\ 1 + \Delta K_{ay} \\ (1 + \Delta K_{ay})\Delta\theta_{x0} \\ (1 + \Delta K_{ay})\Delta\theta_{y0} \\ (1 + \Delta K_{ay})\Delta\theta_{x6} \\ (1 + \Delta K_{ay})\beta_{x1} \\ (1 + \Delta K_{ay})(\beta_{z1} + \Delta\theta_{z3}) \\ (1 + \Delta K_{ay})(\beta_{z1} + \Delta\theta_{z5}) \\ 1 + \Delta K_{az} \\ (1 + \Delta K_{az})\Delta\theta_{x0} \\ (1 + \Delta K_{az})\Delta\theta_{y0} \\ (1 + \Delta K_{az})(\gamma_{y1} + \Delta\theta_{y3}) \\ (1 + \Delta K_{az})(\gamma_{y1} + \Delta\theta_{y5}) \\ (1 + \Delta K_{az})(\gamma_{x1} + \Delta\theta_{x2}) \\ (1 + \Delta K_{az})(\gamma_{x1} + \Delta\theta_{x4}) \\ B_{ax} \\ B_{ay} \\ B_{az} \end{bmatrix} + \varepsilon \quad (18)$$

where  $A$  is a  $72 \times 24$  structure matrix containing only elements 0, 1, and -1, and its rank is 24. Therefore,  $\det(A^T A) \neq 0$  and the parameters  $\Delta K_{ax}$ ,  $\Delta K_{ay}$ ,  $\Delta K_{az}$ ,  $B_{ax}$ ,  $B_{ay}$ ,  $B_{az}$ ,  $\Delta\theta_{x0}$ ,  $\Delta\theta_{y0}$ ,  $\Delta\theta_{y6}$ ,  $\Delta\theta_{z4}$ ,  $\Delta\theta_{x6}$ ,  $\alpha_{y1}$ ,  $\alpha_{z1}$ ,  $\beta_x$ ,  $\beta_{z1} + \Delta\theta_{z3}$ ,  $\beta_{z1} + \Delta\theta_{z5}$ ,  $\gamma_{y1} + \Delta\theta_{y3}$ ,  $\gamma_{y1} + \Delta\theta_{y5}$ ,  $\gamma_{x1} + \Delta\theta_{x2}$ ,  $\gamma_{x1} + \Delta\theta_{x4}$  can be identified using the least squares method.

Since the Earth's rotation rate is too small to provide effective excitations for the three hemispherical resonator gyroscopes of the strapdown inertial navigation system, a set of 48 rotations was designed to serve as the input excitation for the three HRGs.

The procedure involves aligning the  $x_b$ ,  $y_b$ ,  $z_b$  axes of the hexahedral coordinate system upwards and downwards, and then consecutively rotating the hexahedron coordinate system by  $90^\circ$  about the slab's normal vector. Each face of the hexahedron is placed tightly against the located block. Figure 5 illustrates the rotation procedure when the  $z_b$  axis is directed toward the up and down.

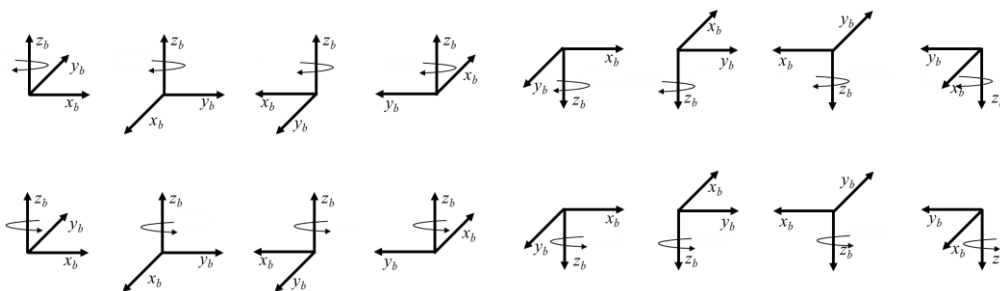


Figure 5. Rotation calibration.

By performing the rotations sequentially, the angular input of the HRG aligned with the  $z$ -axis can be obtained as follows:

$$\begin{aligned}
\alpha_z^{1.5.4} &= \frac{\pi}{2} + \Delta\theta_{z4} - \Delta\theta_{z5} + \omega_{ie}T \sin L \\
\alpha_z^{1.4.3} &= \frac{\pi}{2} + \Delta\theta_{z3} - \Delta\theta_{z4} + \omega_{ie}T \sin L \\
\alpha_z^{1.3.2} &= \frac{\pi}{2} - \Delta\theta_{z3} + \omega_{ie}T \sin L \\
\alpha_z^{1.2.3} &= -\frac{\pi}{2} + \Delta\theta_{z3} + \omega_{ie}T \sin L \\
\alpha_z^{1.3.4} &= -\frac{\pi}{2} - \Delta\theta_{z3} + \Delta\theta_{z4} + \omega_{ie}T \sin L \\
\alpha_z^{1.4.5} &= -\left(\frac{\pi}{2} + \Delta\theta_{z4} - \Delta\theta_{z5}\right) + \omega_{ie}T \sin L \\
\alpha_z^{1.5.1} &= -\left(\frac{\pi}{2} + \Delta\theta_{z5}\right) + \omega_{ie}T \sin L
\end{aligned} \tag{19}$$

By substituting into the gyro error equations of the strapdown inertial navigation system, we can obtain:

$$\begin{bmatrix} g_z^{1.5.4} \\ g_z^{1.4.3} \\ g_z^{1.3.2} \\ g_z^{1.2.5} \\ g_z^{1.2.3} \\ g_z^{1.3.4} \\ g_z^{1.4.5} \\ g_z^{1.5.1} \end{bmatrix} = A \cdot \begin{bmatrix} (1 + \Delta K_{gz}) \cdot \frac{\pi}{2} \\ (1 + \Delta K_{gz}) \cdot \Delta\theta_{z3} \\ (1 + \Delta K_{gz}) \cdot \Delta\theta_{z4} \\ (1 + \Delta K_{gz}) \cdot \Delta\theta_{z5} \\ (1 + \Delta K_{gz}) \cdot (\omega_{ie}T \sin L) + B_{gz} \end{bmatrix} \tag{20}$$

Through the 48 rotation procedures designed in this paper, the relevant error parameters  $\Delta K_{gx}$ ,  $\Delta K_{gy}$ ,  $\Delta K_{gz}$ ,  $B_{gx}$ ,  $B_{gy}$ ,  $B_{gz}$ ,  $\Delta\theta_{x2}$ ,  $\Delta\theta_{x4}$ ,  $\Delta\theta_{x6}$ ,  $\Delta\theta_{y3}$ ,  $\Delta\theta_{y5}$ ,  $\Delta\theta_{y6}$ ,  $\Delta\theta_{z3}$ ,  $\Delta\theta_{z4}$ ,  $\Delta\theta_{z5}$ , can be identified.

By analyzing the outputs of the hemispherical resonator gyroscopes that are perpendicular to the z-axis during the 48 rotation procedures, the relevant errors,  $\alpha_z, \alpha_y, \beta_z, \beta_x, \gamma_y, \gamma_x$ , of the three hemispherical resonator gyroscopes in the strapdown inertial navigation system can be identified.

By substituting the identified hexahedron errors into the accelerometer error model of the strapdown inertial navigation system, the relevant errors of the three accelerometers in the system can be identified.

#### 4. Experimental and Verifications.

An error calibration experiment for the hemispherical resonator gyroscope-based strapdown inertial navigation system was conducted on a three-axis turntable. The turntable was used to simulate the hexahedron structural errors of the strapdown inertial navigation system, and the proposed calibration method was applied to identify the error model parameters of the system. The results are shown in Table 1.

Table 1. Experimental results.

Parameter	Calibration value	Test value	Test deviation
$\Delta K_{ax}$ (ppm)	347.826	351.298	3.472
$\Delta K_{ay}$ (ppm)	512.394	509.780	-2.614
$\Delta K_{az}$ (ppm)	589.173	596.358	7.185
$B_{ax}$ ( $\mu$ g)	431.645	430.698	-0.947
$B_{ay}$ ( $\mu$ g)	624.435	629.466	5.031
$B_{az}$ ( $\mu$ g)	748.815	750.691	1.876
$\alpha_{z1}$ (")	1342.7	1340.4	-2.3
$\alpha_{y1}$ (")	987.4	988.1	0.7

$\beta_{z1}(\prime\prime)$	421.6	423.4	1.8
$\beta_{x1}(\prime\prime)$	725.9	725.4	-0.5
$\gamma_{x1}(\prime\prime)$	1113.2	1112.0	-1.2
$\gamma_{y1}(\prime\prime)$	289.5	290.6	1.1
$\Delta K_{gx}(\text{ppm})$	284.517	282.201	-2.318
$\Delta K_{gy}(\text{ppm})$	397.862	398.351	0.489
$\Delta K_{gz}(\text{ppm})$	465.309	464.285	-1.024
$B_{gx}(\text{°/h})$	0.17248	0.17284	0.00036
$B_{gy}(\text{°/h})$	0.19837	0.19712	-0.00125
$B_{gz}(\text{°/h})$	0.25461	0.25545	0.00084
$\alpha_z(\prime\prime)$	1423.6	1421.9	-1.7
$\alpha_y(\prime\prime)$	879.4	879.7	0.3
$\beta_z(\prime\prime)$	305.7	306.6	0.9
$\beta_x(\prime\prime)$	1167.2	1164.8	-2.4
$\gamma_x(\prime\prime)$	478.9	479.7	0.8
$\gamma_y(\prime\prime)$	1320.1	1318.6	-1.5



**Figure 6.** Experiment.

When the hexahedral structure of the strapdown inertial navigation system based on HRG is free of errors, the calibration errors of each error parameter in the new model and the traditional model are of the same order of magnitude, and there is no significant difference between their calibration results. However, when structural errors exist in the hexahedral structure of the strapdown inertial navigation system, the calibration errors of each error parameter in the traditional model increase by an order of magnitude compared with those in the new model. Moreover, before and after the introduction of structural errors, the calibration errors of each parameter in the new model remain within the same order of magnitude, indicating that the calibration results of the model parameters in the new model are not affected by the structural errors of the strapdown inertial navigation system's hexahedral structure.

## 5. Conclusions

This paper presents a comprehensive on-field calibration method for strapdown inertial navigation systems based on hemispherical resonator gyroscopes, which reduced the influence of the structural errors of the hexahedral on the calibration accuracy of the SINS. A comprehensive error model for the on-field calibration of strapdown inertial navigation systems based on hemispherical resonator gyroscopes was established, and test plan were designed based on this error model. The proposed 24-position accelerometer calibration and 48-rotation gyro calibration schemes allow for simultaneous and accurate identification of sensor biases, scale factor errors, installation misalignments, and fixture-induced structural errors, providing a complete solution for high-precision SINS calibration.

Experimental validation on a high-precision three-axis turntable demonstrates that the proposed method significantly improves the calibration accuracy for both accelerometers and HRGs compared to conventional approaches, while maintaining robustness throughout different orientations and operating conditions. Furthermore, by calibration for the structural errors, the method reduces the mechanical precision requirements for the hexahedral fixture, lowering both the cost and complexity of on-field calibration. Overall, this study provides a robust and practical framework for high-precision calibration of HRG-based SINS and offers a methodology that can be extended to other advanced inertial navigation systems requiring accurate error modeling.

**Funding:** This work was supported in part by the Young Elite Scientist Sponsorship Program by the Cast of China Association for Science and Technology under Grant YESS20220704 and in part by the Heilongjiang Postdoctoral Fund by the Heilongjiang Human Resources and Social Security Bureau of China under Grant LBH-Z22134.

## References

1. Bailey, F. N. Strapdown Calibration and Alignment Study. NASA-ERC Report, Univac Federal Systems Division, 1970.
2. Nassar, S. Improving the Inertial Navigation System (INS) Error Model. Ph.D. Thesis, University of Calgary, Canada, 2003.
3. El-Sheimy, N., Naser, E., & Chiang, K. W. "Inertial sensor calibration for navigation applications: A survey." *Sensors*, 2020, 20(2): 447.
4. Vasconcelos, J., et al. "In-field calibration of low-cost inertial and magnetic sensors." *IEEE Transactions on Instrumentation and Measurement*, 2011, 60(6): 2154–2164.
5. Nieminen, T., et al. "Calibration of consumer-grade MEMS IMUs using multi-position and rotation methods." *IEEE Sensors Journal*, 2014, 14(11): 3751–3762.
6. Rahimi, H., et al. "Improving the calibration process of inertial measurement units for marine navigation." *Navigation*, 2020, 67(4): 763–770.
7. Vavilova, N. B. "The calibration problem in inertial navigation." *Journal of Applied Mathematics and Mechanics*, 2021, 85(3): 263–272.
8. Ruan, S., Guo, X., Shao, H., Liu, J., & Tu, Z. "Hexahedral prism and IMU installation error calibration technique based on turntable transmission." *IOP Conf. Ser.: Earth Environ. Sci.*, 2020, 502: 012013.
9. Zhang, J., et al. "Improved external-field calibration method for strapdown INS considering fixture misalignments." *IEEE Transactions on Aerospace and Electronic Systems*, 2022, 58(5): 3810–3823.
10. Li, Y., Zhang, W., & Chen, Q. "Error modeling and compensation of hexahedral fixture misalignments in inertial navigation calibration." *Measurement Science and Technology*, 2023, 34(7): 075102.

**Disclaimer/Publisher's Note:** The statements, opinions and data contained in all publications are solely those of the individual author(s) and contributor(s) and not of MDPI and/or the editor(s). MDPI and/or the editor(s) disclaim responsibility for any injury to people or property resulting from any ideas, methods, instructions or products referred to in the content.